DAHLGREN DIVISION
NAVAL SURFACE WARFARE CENTER

Silver Spring, Maryland 20903-5640

NSWCDD/TR-95/187

MICROWAVE PROBE FOR MASS MEASUREMENTS OF A WATER PLUME

BY J. Y. CHOE, K. A. BOULAIS, S. T. CHUN, AND K. A. IRWIN

SYSTEMS RESEARCH AND TECHNOLOGY DEPARTMENT

30 SEPTEMBER 1995

REPORT DOCUMENTATION PAGE

Form Approved
OBM No. 0704-0188

1. AGENCY USE ONLY (*Leave blank*)	2. REPORT DATE	3. REPORT TYPE AND DATES COVERED
	30 September 1995	Final

4. TITLE AND SUBTITLE
MICROWAVE PROBE FOR MASS MEASUREMENTS OF A WATER PLUME

5. FUNDING NUMBERS
---

6. AUTHOR(s)
J. Y. Choe, K. A. Boulais, S. T. Chun, and K. A. Irwin

7. PERFORMING ORGANIZATION NAME(S) AND ADDRESS(ES)
Naval Surface Warfare Center Dahlgren Division
White Oak Detachment (Code B42)
10901 New Hampshire Avenue
Silver Spring, MD 20903-5640

8. PERFORMING ORGANIZATION REPORT NUMBER
NSWCDD/TR-95/187

9. SPONSORING/MONITORING AGENCY NAME(S) AND ADDRESS(ES)
Office of Naval Research (ONR 351)
Ballston Centre Tower One
800 North Quincy Street
Arlington, VA 22217-5660

10. SPONSORING/MONITORING AGENCY REPORT NUMBER
---

11. SUPPLEMENTARY NOTES

12a. DISTRIBUTION/AVAILABILITY STATEMENT
Approved for public release; distribution is unlimited.

12b. DISTRIBUTION CODE
---

13. ABSTRACT (Maximum 200 words)

The use of water plumes produced by shallow underwater explosions is being studied as an effective, low cost defense of ships against low flying missiles. The key element for the success of this concept is the total water mass contained within the plume. An experimental program has been conducted to measure the plume water mass in situ since no previous data exist relative to this ship self defense concept. Here we describe a microwave probe that was used to measure the amount of water in the plume. The method is based on the attenuation characteristics of a microwave beam that has been propagated through the plume. The attenuation coefficient can be obtained by measuring the amplitude of the wave after traversing the plume. This information can then be used to derive the water density since the attenuation characteristics depend only on the macroscopic volume ratio of water to air. In this paper, we first formalize the theory relating the water density to the microwave attenuation rate. After the experimental implementation of the theory has been laid out, specific experimental results from the actual field tests are presented.

14. SUBJECT TERMS
Water Plume, Shallow Underwater Explosion, Water Plume Volume Density, Microwave Probe, Microwave Beam Attenuation, Field Tests, Equivalent Water Length

15. NUMBER OF PAGES
23

16. PRICE CODE

17. SECURITY CLASSIFICATION OF REPORT	18. SECURITY CLASSIFICATION OF THIS PAGE	19. SECURITY CLASSIFICATION OF ABSTRACT	20. LIMITATION OF ABSTRACT
UNCLASSIFIED	UNCLASSIFIED	UNCLASSIFIED	SAR

FOREWORD

This work was supported by the Venture Fund of the Naval Surface Warfare Center, Dahlgren Division (NSWCDD). The field tests were supported by the Office of Naval Research, Code ONR 351.

The field test participants were the authors (Electromagnetics Group, NSWCDD Code B42), Charles Higdon, (NSWCDD Code G23), Len Lipton (Naval Surface Warfare Center Indian Head Division [NSWCIHD] Code 450), and Joe Connor (NSWCIHD Code 950). The numerical simulation work was performed by William Szymczak (NSWCDD Code B44).

Approved by:

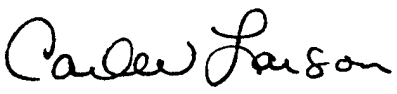

CARL LARSON, Head
Physics and Technology Division

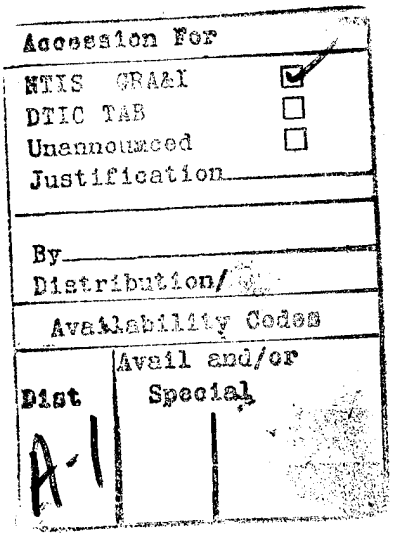

CONTENTS

ILLUSTRATIONS

CHAPTER 1

INTRODUCTION

The Water Barrier Ship Self-Defense Concept[1,2] has been proposed at the Naval Surface Warfare Center, Dahlgren Division (NSWCDD) as a means to provide a low cost but effective defense against high speed, low flying anti-ship missiles (ASMs). The scheme utilizes a multitude of shallow underwater explosions, each creating a plume of water yielding a wide barrier between the ship and the threat. The barrier protects the ship by one or more methods. First, it masks the ship simply by slowing or stopping the attacking ASMs. Second, it stops fragments from missiles previously killed at short range. Finally, it may defeat the fuzing and structure of an ASM that attempts to penetrate the self defense layer. A key issue of this concept is the amount of water that the ASM would interact with, and its relation to these three defense mechanisms. In this paper, we discuss a measurement scheme[3] used to determine the amount of water in the barrier based on microwave absorption. For a more in-depth discussion of the Water Barrier Ship Self-Defense Concept, the reader is referred to References 1 and 2.

As previously mentioned, the principal quantity of interest for the concept is the water mass contained within the plume since this is what renders the necessary mechanical impact to the missiles. In particular, it is necessary to be able to reasonably predict the water plume mass as a function of explosive system parameters including the weight, depth, and spatial density of the charges. To this end, a program was set up to devise measurement methods to quantify the water plume mass experimentally in scaled-down, but realistic situations.

Unfortunately, no prior methodology existed for the experimental measurement of the water mass of plumes generated by shallow underwater explosions. There have been numerous data reported for rain and fog,[4] but their densities are far less than those of the water plumes that we are experiencing. To put this in perspective, a crude calculation indicates that a plume relevant to our scaled-down case is approximately equivalent to a rate of 10^4-10^5 mm/hr of rain. Compare this to a tropical downpour that typically has a rate in the order of tens of mm/hr. As a result, new measurement techniques had to be developed for the barrier concept. The NSWC experiment[3] employed two different methods to measure the mass density of the water plume: (1) a probe based on microwave absorption, and (2) a conductivity probe method.[5] The density measured from the two experimental approaches were then compared to that from a hydrodynamic computer simulation of the plumes.[6] The conductivity probe method, which yielded spatially resolved data, will be explained elsewhere.[5] In this report we will concentrate only on the microwave method.

The basic concept of the microwave probe as applied in this case comes from the recognition of the water plume as a mixture of water and air. Specifically, we maintain that, at the microwave frequencies, the wavelength is much larger than the water droplet size. In this macroscopic domain, the two media appear as a single material through which the microwaves will pass and the size and shape of the individual water droplets is no longer of concern. More precisely, the propagation characteristics of the mixture (i.e., plume) depend only on the global density. In particular, there exists a one-to-one correspondence between the microwave absorption and the relative volume density of the plume. Thus, once the propagation characteristics are known, the plume density may be uniquely determined.

In Chapter 2 we present the theory of the microwave probe method. The relationship between the water mass density of the plume and the microwave propagation characteristics is derived. The experimental setup, together with the procedure to extract the mass density data, will be given in Chapter 3. Experimental results are presented in Chapter 4.

CHAPTER 2

THEORY

Consider the relative size of the water droplets in a plume, and their separation, as compared to the wavelength of the propagating electromagnetic wave (Figures 1(a) and 1(b)). The plume, when viewed within the visible spectrum, can be seen as water droplets within a background of air. Both the water and air maintain their own respective material characteristics. When the wavelength is smaller than or comparable to the water droplet size, the shapes and locations of the water droplets individually affect the wave propagation properties through multiple scattering and irregular refraction. The wave *sees* the microscopic quantities of the water particles. This case is depicted in Figure 1(a).

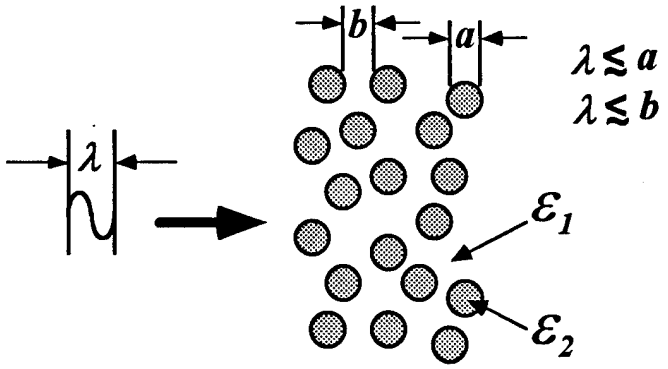

(a) Where the wave is affected by the individual particles that are larger than the wavelength.

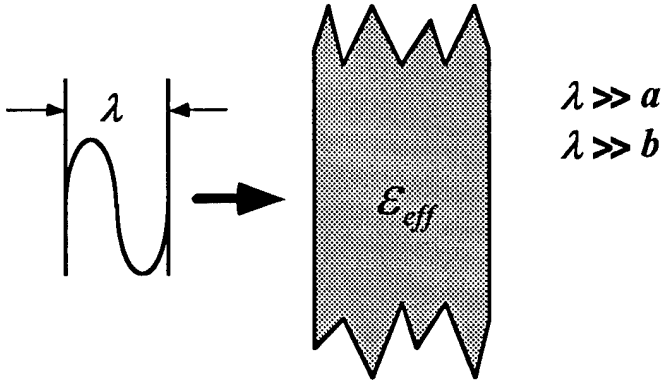

(b) Where a mixture's propagation characteristics seem uniform to the longer wavelength wave.

FIGURE 1. RELATIONSHIP BETWEEN WAVELENGTH AND PARTICLE SIZE

Conversely, when the wavelength is much longer than the droplet size and separation, the mixture appears to be uniform. This is generally the case for microwaves and is shown in Figure 1(b). The electromagnetic propagation characteristics are distinct from either pure air or pure water. This "new" medium loses its microscopic quantities such as particle shape, size, and distribution and instead keeps only macroscopic quantities such as density and temperature.

The appearance of a uniform medium is beneficial since the propagation properties of an electromagnetic wave now depend only on the material's composition. In fact, there exists a one-to-one correspondence between the propagation characteristics of the combined medium and its average water density. From an experimental viewpoint, an attenuation measurement can be used to uniquely determine the water density integrated over the electromagnetic beam size. This relationship between the attenuation rate and the water density is the basis for the microwave probe system and can be derived as follows.

We assume plane wave propagation such that the electric (**E**) and magnetic (**H**) fields can be described as

$$\begin{pmatrix}\mathbf{E}\\ \mathbf{H}\end{pmatrix} = \begin{pmatrix}\mathbf{E}_0\\ \mathbf{H}_0\end{pmatrix} \exp(-j\beta z + j\omega t) \tag{1}$$

where ω is the angular frequency and β is the propagation wavenumber in the direction z. The bold typeface represents vector quantities. The dispersion relation between ω and β in the medium of interest can be given by

$$\beta^2 = \frac{\omega^2}{c^2}\varepsilon\,, \tag{2}$$

where c is the speed of light in vacuum and ε is the dielectric constant of the medium. Generally, ε is complex and can be expressed as

$$\varepsilon = \varepsilon' - j\varepsilon'' = |\varepsilon| \exp(-j\theta) \tag{3}$$

where the magnitude and phase of the dielectric constant can be expressed in terms of the real and imaginary parts as

$$|\varepsilon| \equiv \left[(\varepsilon')^2 + (\varepsilon'')^2\right]^{1/2}, \text{ and } \theta = \tan^{-1}(\varepsilon''/\varepsilon') \tag{4}$$

The relation for the complex dielectric constant, as given by equations (3) and (4), is graphically represented in Figure 2.

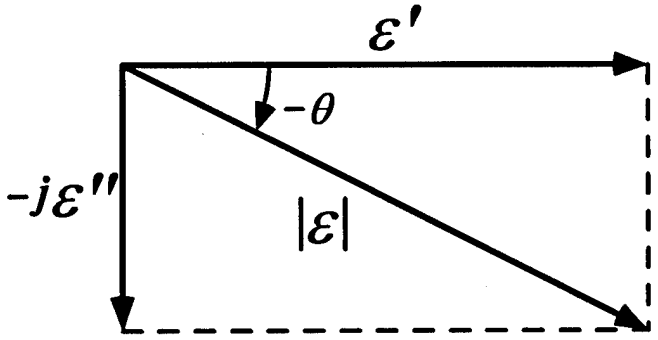

FIGURE 2. REPRESENTATION OF COMPLEX DIELECTRIC CONSTANT

In terms of the complex dielectric constant, the dispersion relation can now be written as

$$\beta = \beta' - j\beta'' = \frac{\omega}{c}|\varepsilon|^{1/2} \exp\left(-j\frac{\theta}{2}\right) \quad . \tag{5}$$

Thus, the spatial dependence of the electric field (and similarly the magnetic field) now becomes

$$|\mathbf{E}|(z) = |\mathbf{E}|(z=0) \cdot \exp(-\beta'' z) \tag{6}$$

which represents a damped wave. Since the power, P, within the wave is proportional to the square of the field, we have

$$\mathrm{P}(z) = \mathrm{P}(z=0) \cdot \exp(-\alpha z) \tag{7}$$

where the attenuation coefficient is given purely in terms of the imaginary part of β as

$$\alpha = 2\beta'' = \frac{2\omega}{c}|\varepsilon|^{1/2} \cdot \sin\left(\frac{\theta}{2}\right) \quad . \tag{8}$$

Note that the real part of β will generally affect the propagation characteristics of the wave as well. This is particularly true at the boundary where the wave propagates from one macroscopic medium into another and the real part of β for one medium is significantly different from the other. In such a case, one can expect scattering and refraction of the wave. However, the density of the plume is low enough that the real part of β is sufficiently close to that of air, which allows the effects to be neglected.

The dispersion relation of equation (8) states that once the complex dielectric constant of the medium is known, so are all of the propagation characteristics of the electromagnetic wave. Therefore, if the attenuation coefficient of the wave, α, can be measured, then one can predict the

dielectric constant, ε. We intend to find a quantitative relationship between the dielectric constant of the plume and the total water volume, V_w, from which the water density can be extracted.

The effective dielectric constant for a uniform mixture of more than one material has been studied before.[7] If a medium is composed of two materials with different dielectric constants given by ε_1 and ε_2 (refer to Figure 1), then the *effective* dielectric constant is given by

$$\varepsilon_{eff} = \varepsilon_1^{V_1} \cdot \varepsilon_2^{V_2} \quad , \tag{9}$$

where it is assumed that the wavelength of the electromagnetic wave is much greater than the particle size and the spacing of either material. In equation (9), V_1 and V_2 are the volume ratios corresponding to each material such that

$$V_1 + V_2 = 1 \quad . \tag{10}$$

Equation (9) becomes applicable to the plume experiments by assigning the water droplets as one material and the air between them as the other material. However, some comments are required since equation (9) was originally derived for the case in which both dielectric constants were real (i.e., without dissipation) whereas, for water, the dielectric constant is complex. Before invoking an analytical continuation[8] by extending the valid region of equation (9) off the real axis into the complex plane (see Figure 2), one has to remove any ambiguity in the arguments of the complex quantities. As shown in Figure 2, the argument of the dielectric constant, θ, is physically unique with the restriction $0 \le \theta < \pi/2$. Thus, one can extend the relationship of equation (9) to include a complex dielectric constant since θ can be measured uniquely. For the plume, equation (9) then reduces to

$$\varepsilon_p = \varepsilon_w{}^{V_w} \tag{11}$$

where we have used the good approximation that the complex dielectric constant of air is unity. In equation (11), the subscript p (w) refers to the plume (water) quantities. That the dielectric constant for pure water is complex allows us to write

$$\varepsilon_w = \varepsilon_w{}' - j\varepsilon_w{}'' \equiv |\varepsilon_w| \cdot \exp(-j\theta_w) \tag{12}$$

where again the magnitude and phase can be related to the real and imaginary parts through

$$|\varepsilon_w| = \left[(\varepsilon_w{}')^2 + (\varepsilon_w{}'')^2 \right]^{1/2}, \quad \theta_w = \tan^{-1}\left(\frac{\varepsilon_w{}''}{\varepsilon_w{}'} \right) \quad . \tag{13}$$

By using equations (11) and (12) in (8), the attenuation coefficient of a plume, normalized to that of pure water ($V_w = 1$), can be found as

$$\hat{\alpha} \equiv \frac{\alpha_p}{\alpha_w} = \frac{|\varepsilon_w|^{V_w/2}}{|\varepsilon_w|^{1/2}} \cdot \frac{\sin\left(\frac{V_w}{2}\theta_w\right)}{\sin\left(\frac{1}{2}\theta_w\right)} \tag{14}$$

where α_p is the attenuation coefficient of the plume, and the normalization constant is

$$\alpha_w = \frac{2\omega}{c} \cdot |\varepsilon_w|^{1/2} \sin\left(\frac{1}{2}\theta_w\right) \quad . \tag{15}$$

Equation (14) is a direct relationship between the attenuation coefficient and the water volume ratio V_w, and is a function only of the complex dielectric constant of 100% water, which is well known. However, equation (14) cannot be inverted in closed form for V_w in terms of α_p as experimentally required. Instead of using an iterative approach, equation (14) can be inverted by taking advantage of several simplifying approximations. In the limit that V_w is close to zero, the power function in equation (14) can be Taylor expanded to second order resulting in a quadratic function given by

$$V_w = \frac{\left[1 + 2\hat{\alpha}|\varepsilon_w|^{1/2} \cdot \ln|\varepsilon_w| \frac{\sin\left(\frac{\theta_w}{2}\right)}{\left(\frac{\theta_w}{2}\right)}\right]^{1/2} - 1}{\ln|\varepsilon_w|}, \quad as\ V_w \to 0 \quad . \tag{16}$$

A further approximation is possible since the loss tangent of water, θ_w, is small (i.e., $\varepsilon_w'' << \varepsilon_w'$) further reducing equation (16) to

$$V_w = \frac{\left[1 + 2\hat{\alpha}|\varepsilon_w|^{1/2} \cdot \ln|\varepsilon_w|\right]^{1/2} - 1}{\ln|\varepsilon_w|}, \quad as\ V_w,\ \theta_w \to 0 \quad . \tag{17}$$

Both approximations are reasonable for the plume densities and microwave frequencies encountered in this work. Figure 3 is a plot of the normalized attenuation coefficient as a function of water volume ratio for the approximate equations (16) and (17) as compared to the exact equation (14). The plots were generated using ε_w'=71.8 and ε_w''=16.15 corresponding to the real and imaginary parts of the dielectric constant for pure water as consistent with the experimental setup (see Chapter 3). From the graph, note that the two approximations are nearly indistinguishable. Further, the water volume ratio of the plumes used in this work was below 10% of the total plume volume and, at V_W = 0.1, equation (17) represents an error in $\hat{\alpha}$ of only 2.3%

from the exact equation (14). Thus, the two approximate equations provide acceptable means, and the quadratic expression in V_W confirms experimental results published elsewhere.[4]

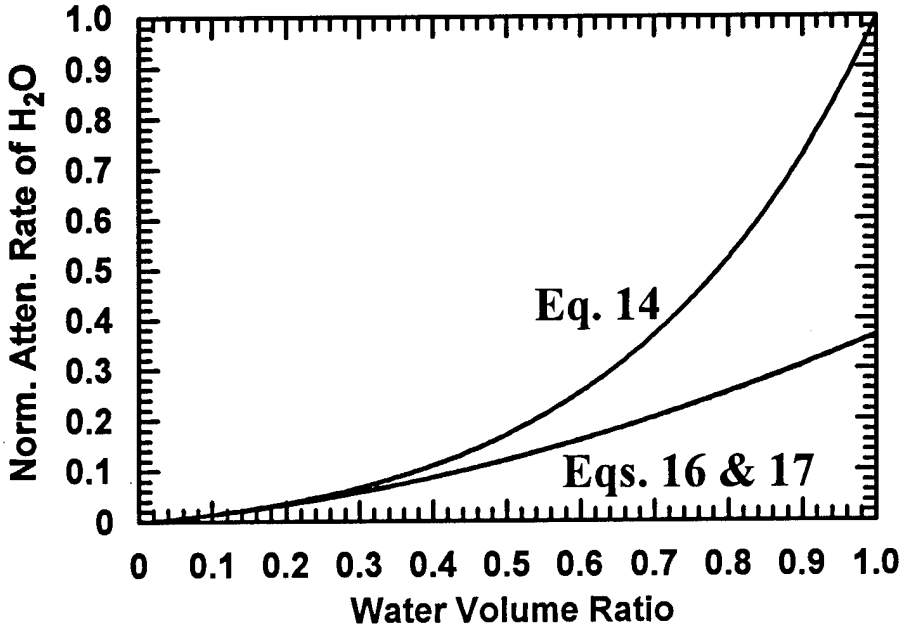

FIGURE 3. NORMALIZED ATTENUATION COEFFICIENT AS A FUNCTION OF WATER VOLUME RATIO

Several other points can be made from Figure 3. Although the validity becomes questionable as the water density increases, equation (14) recovers the correct attenuation coefficient at 100% water density (i.e., $\alpha_p = \alpha_w$ at $V_W = 1$). In the intermediate range, however, the attenuation curve is not linear. This means that the attenuation of the water/air mixture is not linear with density but instead is reduced at the lower densities. In fact, we can construct a curious hypothetical situation: consider a microwave signal passing through two different plumes, one with a path length L and a uniform density V_W, and the other with a $2L$ path length and a density of $V_W/2$. Although the microwave is passing through the same amount of total water, the resulting attenuation is less for the lower density and longer path length case (i.e., $\alpha(V_w)\cdot L > \alpha(V_w/2)\cdot 2L$). This seemingly peculiar effect comes from the fact that the effect of the water is appreciable only as the density approaches pure water.[7]

CHAPTER 3

EXPERIMENTAL APPROACH

A simplified experimental arrangement is given in Figure 4. A transmitter (T_x) and receiver (R_x) are located on either side of the plume (only the antennas are shown). The microwave beam propagates horizontally through the plume at a height of 25 feet. A pulsed traveling wave tube (TWT) operating at a frequency of 4.000 GHz and a power of 1 kW was used as the transmitter. The choice of frequency will be discussed subsequently in more detail. A pulse width of 10 μs with a repetition frequency of 1 kHz was used allowing a more than adequate sampling rate relative to the motion of the plume. The transmitting antenna was a parabolic dish 6 feet in diameter. The receiver used an identical antenna that fed the attenuated signal into a direct-coupled log video amplifier (DLVA) capable of a 51 dB dynamic range. Timing control was accomplished using a pulse generated at the transmitter via direct cable link to the receiver. At the receiver, the signals were amplified and buffered before being recorded by a data acquisition system. The antennae were separated by a distance of 270 feet with the plume centered about the halfway point.

For a circular antenna aperture with tapered illumination, the Fresnel-Fraunhofer transition point is 57.5 feet. Thus, the plume occurred past the radiation mid-field where the beam does not spread appreciably. Throughout our analyses, the spatial variations in the plume perpendicular to the microwave beam direction are assumed negligible over the cross section of the microwave beam. This is due, in part, to the fact that the microwave beamwidth was much smaller than the plume width (typically less than 10%) and, in part, to the low water density of the plume. Furthermore, because of the lower plume water density, we may assume that at any given time, α_p is nearly constant within the plume in the propagating direction, z. Thus, the received power from equation (7) can be represented by

$$P_{R_x}(t) = P_{R_x}(0) \cdot \exp\left[-\left\langle \alpha_p(t) \right\rangle L(t)\right] \tag{18}$$

where P_{R_x} (0) is the received power level at t=0 in the absence of a plume, and the < > bracket represents an average value. The required path length through which the microwave beam traverses the plume, $L(t)$, was measured via video camera. Note that the received power is a function of the product of the average attenuation coefficient and this propagation length, as opposed to the attenuation coefficient only. This must be taken into account when applied to equation (17). Figure 5 presents a representative signal recorded at the receiver. As the plume density becomes larger, the attenuation increases and the received power level drops.

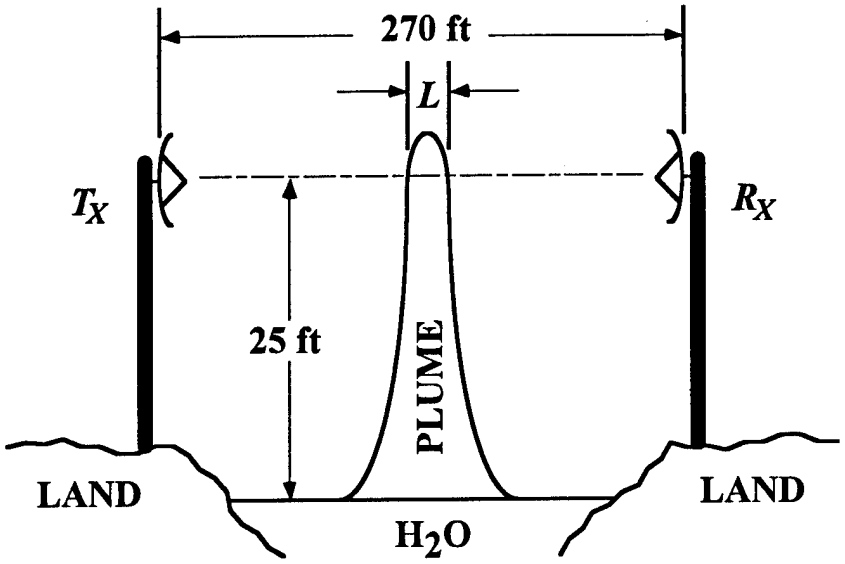

FIGURE 4. SCHEMATICS OF MICROWAVE PROBE SYSTEM SETUP

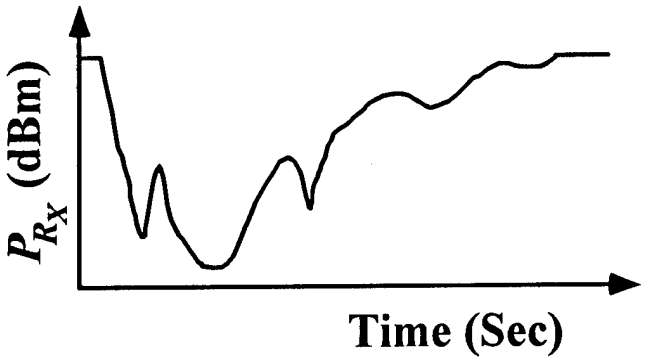

FIGURE 5. SCHEMATIC DATA OF RECEIVED POWER AS A FUNCTION OF TIME

To first order, the most important quantity for the Water Barrier Ship Self-Defense Concept[1,2] is the total water mass that a missile would see as it propagates through the plume. Thus, we have devised a quantity that represents an equivalent length of 100% water, which we call the equivalent water length, EWL. The EWL can be found by simply multiplying the resultant water volume ratio given by equation (17) by the plume length given by

$$\mathrm{EWL}(t) = \langle V_w(t) \rangle \cdot L(t) \tag{19}$$

In practice, one would first solve for the average attenuation from the raw data as a function of time using equation (18). This attenuation would then be applied to equation (17) via equation (14) to obtain the water volume density. Finally, equation (19) would be used, again

with $L(t)$, to obtain the EWL. Figure 6 is a representation of the final EWL resulting from the schematic data of Figure 5.

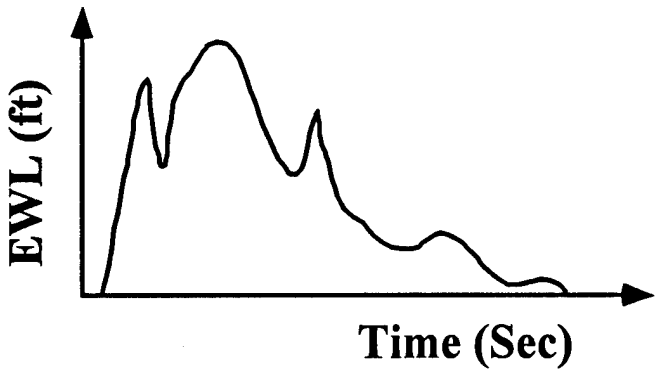

FIGURE 6. FINAL RESULT OF TIME-RESOLVED EQUIVALENT WATER LENGTH OF THE PLUME

Several comments are in order here. First, note from Figure 3 that the attenuation rate is represented on a logarithmic scale, while the water volume ratio is in linear units. This is also true in both Figures 5 and 6. This means that if a 40 dB dynamic range detector was needed to measure a 5% water density, then a detector capable of more than 80 dB would be required to measure a 10% water density. Thus, the microwave probe is limited by the dynamic range of the detector, which falls off quickly. However, the system is quite useful for plume densities that are not excessive. Also, the lower density plume has the advantage in that the EWL becomes nearly independent of the path length, $L(t)$.

We are now in a position to discuss our choice of microwave frequency. Several parameters were considered, including the attenuation rate of the microwave beam within the plume, the practical size of the antennae, and the propagation range. A practical compromise was used in the final design parameters. First, the attenuation of the microwaves traversing the plume is a strong function of frequency. The loss tangent (defined by $\varepsilon''/\varepsilon'$) for 100% water[9] is plotted as a function of microwave frequencies at various water temperatures in Figure 7. There is a resonance near 10 GHz, from which the attenuation remains high down to a frequency of about 1 GHz. Of course, the plume is significantly less than 100% water density, yielding a much lower attenuation rate than displayed in Figure 7. However, with $L(t)$, the total attenuation is still large and it is prudent to avoid frequencies of high attenuation rates. From this perspective, it is desirable to use a frequency near 1 GHz. On the other hand, the microwave beam needs to be reasonably focused when it reaches the plume to preserve spatial resolution and power, which means that the size of the antenna has to be large compared to its wavelength. This fact favors higher frequencies for practical antenna sizes. Another consideration which supports the use of higher frequencies is that a well-defined beam was assumed in the development of the theory, requiring the plume to be past the Fresnel-Fraunhofer transition point which, in turn, is proportional to frequency. Considering these factors, along with cost and availability, a frequency of 4.000 GHz was selected. During our measurements, the water temperature was measured to be 30 °C, requiring an interpolation of the data of Figure 7.

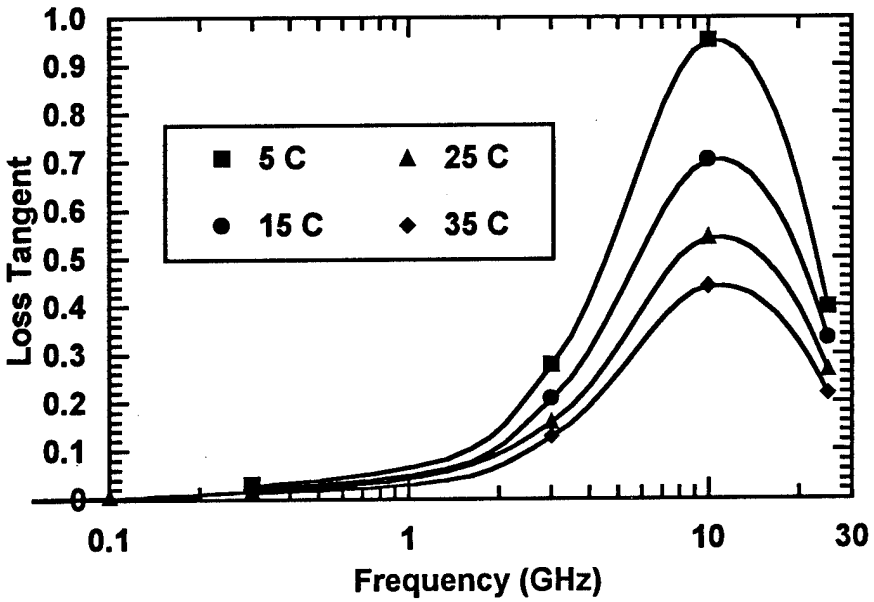

FIGURE 7. LOSS TANGENT OF FULL WATER VS. FREQUENCY AT VARIOUS WATER TEMPERATURES

CHAPTER 4

EXPERIMENTAL RESULTS

For a proof-of-concept of the Water Barrier Ship Self-Defense Concept, a small-scale plume test was conducted at the Hi-Test Facility at Arvonia, Virginia, in August 1993. Both single-charge shots and multiple-charge shots were used. The multiple-charge shots consisted of several single charges arranged linearly with various separation distances. Both the charge weight and depth were also varied from shot to shot throughout the test. Each individual charge consisted of 10 pounds of composition C4. Further details are reported elsewhere.[1-3] In this paper, we will give two results from the test. The experimental results are compared to the results of a hydrodynamic numerical simulation.[6] As pointed out in Chapter 3, the relevant quantity is the equivalent water length (EWL) as a function of time. Figure 8 gives the EWL for a single-charge shot. The depth of the charge was 10 feet from the water surface, which was shallow enough to neglect the reflective shock effects of the pond bottom. The experimental data agrees reasonably well with the numerical code both in terms of the magnitude and the time profile.

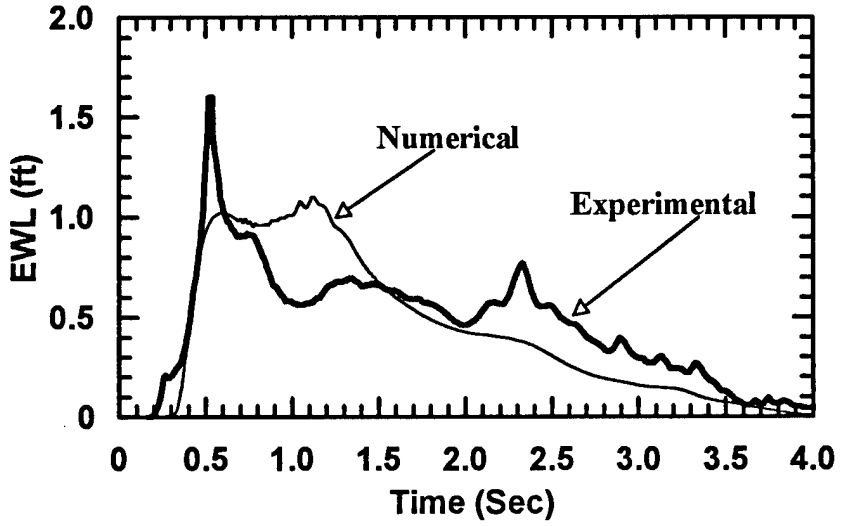

FIGURE 8. COMPARISON OF MICROWAVE PROBE AND NUMERICAL RESULT OF A SINGLE-CHARGE SHOT

For the multiple-charge shots, five charges were arranged so they were perpendicular to the microwave direction. Obviously the multiple-charge shots produced much larger and denser plumes. An example of a multiple-charge shot is presented in Figure 9. Again, the EWL is plotted as a function of time and compared with the numerical result. The microwave data clearly shows

the limit of our setup. The flat top portion of the curve represents a received power level that fell below the noise floor of the detector--that is, the attenuation due to the water plume was greater than the dynamic range of the detector. Again, as mentioned in Chapter 3, the microwave method works well for low density plumes. Nevertheless, by extrapolating the cutoff region and assuming a general trend that follows the single-shot case, one can estimate the peak values and time profiles for the EWL in the multiple-shot cases. With this stated, the comparison with numerical results is again reasonable.

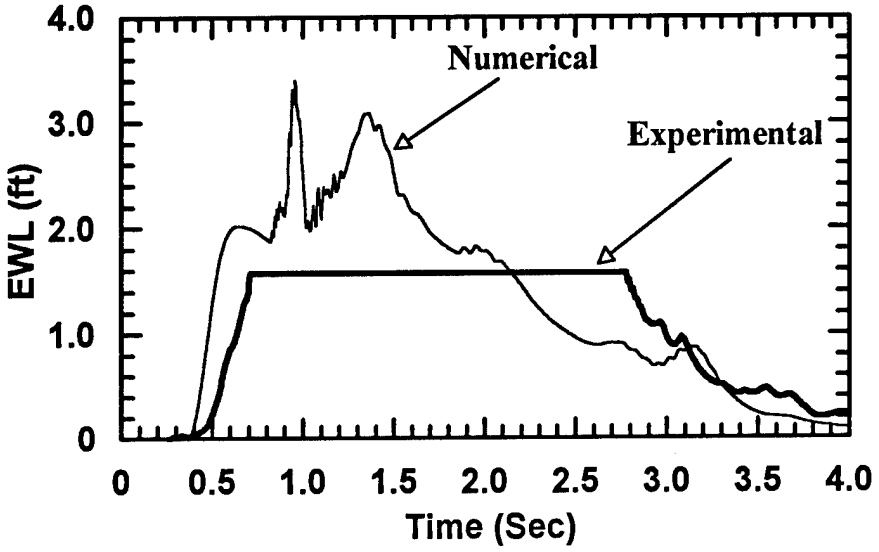

FIGURE 9. COMPARISON OF MICROWAVE PROBE AND NUMERICAL RESULT OF A MULTIPLE-CHARGE SHOT

CHAPTER 5

CONCLUSIONS AND FUTURE WORK

In this paper, a method to measure the water density in a plume created from an underwater explosion has been described. This information is important for the Water Barrier Ship Self-Defense Concept,[1,2] which utilizes such plumes to disable low flying ASMs. Our scheme is based directly on the measurement of the total attenuation of a microwave beam traversing the plume. The plume is considered in terms of its macroscopic quantities due to the larger wavelength of the microwaves in comparison to the water droplet size and separation. Treating the plume as a water-air mixture allows a one-to-one correspondence between the total attenuation and the water volume ratio. Several reasonable assumptions allowed inversion of the nonlinear relation required by the experiment. The theory was developed, and a recipe for converting the measured attenuation to a quantity representing an equivalent amount of 100% water was presented.

Several improvements exist that would enhance the microwave probe measurement scheme. First, several antennas may be used at both the transmitter and receiver to provide perpendicular spatial resolution. Assuming the transmitting source has enough power, only the additional antennas would be required on the transmitting side by prior splitting of the power. Further, by multiplexing the signal at the receiver side, only additional receiving antennas would be required on the receiving end, which saves the cost of expensive detectors. Another improvement can be made in the receiver itself. Current receivers are capable of dynamic ranges of nearly three times that used in this test. Such a receiver would similarly measure EWLs on the order of three times those measured here. These improvements have been planned for future tests.

REFERENCES

1. Higdon, C., *Water Plume Concept for Ship Self Defense*, NSWC TR 91-710, 1992, Naval Surface Warfare Center, Silver Spring, MD.

2. Higdon, C. "Water Barrier Ship Self-Defense Concept," *NSWCDD Technical Digest*, September 1994, Naval Surface Warfare Center Dahlgren Division, Dahlgren, VA, pp. 140-153.

3. Choe, J.; Boulais, K.; Chun, S.; Irwin, K.; Lipton, L.; Szymczak, W.; and Higdon, C., "Mass Measurement of Water Plumes Produced by Underwater Explosion," in *Proceedings Test Symposium*, 1994, Johns Hopkins Applied Physics Laboratory, Laurel, MD, pp. 493-504.

4. Becker, G. E. and Autler, S. H., "Water Vapor Absorption of Electromagnetic Radiation in Centimeter Wave-Length Range," *Phys. Rev.*, Vol. 70, 1945, p. 300.

5. Lipton, L., *Probe for Measurement of Water Mass of Plumes Produced by Underwater Detonation*, IHTR 1757, 1994.

6. Szymczak, W. and Solomon, J., *Computations and Experiments of Shallow Depth Explosion Plumes*, NSWCDD/TR-94/156, 1994, Naval Surface Warfare Center Dahlgren Division, Silver Spring, MD.

7. Reynold, J. A. and Haugh, J. M., "Formulae for Dielectric Constants of Mixtures," *Proc. Phys. Soc.*, Vol. 70, 1957, p. 769.

8. Churchill, R. V.; Brown, J. A.; and Verhey, R. F., *Complex Variables and Applications*, MacGraw-Hill, New York, 1976, Chap. 12.

9. Von Hipple, A., *Dielectric Materials and Applications*, Technology Press of M.I.T. & John Wiley, New York, 1954, p. 361.

DISTRIBUTION

	Copies
DOD ACTIVITIES (CONUS)	
ATTN ONR 351 D SIEGEL CHIEF OF NAVAL RESEARCH BALLSTON CENTRE TOWER ONE 800 NORTH QUINCY STREET ARLINGTON VA 22217-5660	1
ATTN CEWES-SE-R M FORD COMMANDER U S ARMY ENGINEER WATERWAYS EXPERIMENT STATION 3909 HALLS FERRY ROAD VICKSBURG MS 39181	1
ATTN PMS 400 R BRITTON	1
03K1 K LONG COMMANDER NAVAL SEA SYSTEMS COMMAND DEPARTMENT OF THE NAVY NATIONAL CENTER 2 2531 JEFFERSON DAVIS HWY ARLINGTON VA 22242-5160	1
ATTN CODE E29L TECHNICAL LIBRARY COMMANDING OFFICER COASTAL SYSTEMS STATION DAHLGREN DIVISION NAVAL SURFACE WARFARE CTR 6703 W HIGHWAY 98 PANAMA CITY FL 32407-7001	1
DEFENSE TECHNICAL INFORMATION CENTER CAMERON STATION ALEXANDRIA VA 22304-6145	12

	Copies
NON-DOD ACTIVITIES (CONUS)	
THE CNA CORPORATION P O BOX 16268 ALEXANDRIA VA 22302-0268	1
ATTN GIFT AND EXCHANGE DIVISION LIBRARY OF CONGRESS WASHINGTON DC 20540	4
INTERNAL	
NSWCIHDIV PERSONNEL	
450 L LIPTON	1
590 G GESSNER	1
960 J CONNOR	1
NSWCDD PERSONNEL	
B053 R STATON	1
B42 K BOULAIS	3
B42 J CHOE	3
B42 K IRWIN	1
B44 W SZYMCZAK	1
D4 M LACEY	1
E231	3
E232	2
F101 T McCANTS	1
G20 D BRUNSON	1
G23 T RICE	1
G23 C HIGDON	3
G23 G GRAFF	1
G70T R DORCEY	1
N22 L TRIOLA	1
N22 J BURROWS	1
N742 GIDEP	1